Magnetic mineral diagenesis in anoxic laminated sediments from the Southern Gulf of California

LIGIA PÉREZ-CRUZ AND JAIME URRUTIA-FUCUGAUCHI

Laboratorio de Paleoceanografía y Paleoclimas, Instituto de Geofísica, Universidad Nacional Autónoma de México, Ciudad Universitaria, Coyoacan 04510 D.F., Mexico
(perezcruz@igeofisica.unam.mx)

Received: May 29, 2016; Revised: November 25, 2016; Accepted: April 10, 2017

ABSTRACT

Diagenetic effects on the magnetic mineralogy in marine sediments have long been investigated, including oxidation/reduction reactions, magnetic dilution, formation of iron sulfides and oxides, magnetization acquisition mechanisms and reliability of the paleomagnetic record. This study investigates diagenetic effects in low-oxygen depositional environments characterized by recent and past magnetic mineral dissolution zones. We analyze a marine sequence from the Alfonso Basin in the southern Gulf of California in which the topmost sediments show diagenetic effects marked by high magnetic enhancement factors. The susceptibility logs show high values at the top sediments with well-defined small amplitude low frequency fluctuations down core. Magnetic hysteresis loops indicate low coercivity saturation, characteristic of magnetites and low-tititanomagnetites with varying paramagnetic contributions. Intensity of natural remanent, isothermal and anhysteretic magnetizations and coercivity parameters show similar variation patterns with depth. The anhysteretic remanence intensity-susceptibility ratio shows an inverse correlation to magnetic susceptibility, indicating varying concentration of fine grained single domain and superparamagnetic particles. The magnetic logs record diagenetic changes and magnetite authigenesis, with preserved recent and old dissolution zones marked by enriched single-domain/pseudo-single-domain/multi-domain magnetite in between the dissolution fronts. The oxidation/reduction processes relate to climatic and water/sediment interface factors controlling the dissolution processes, which occur in the Alfonso Basin anoxic conditions.

Keywords: sediment diagenesis, magnetic properties, laminated sediments, Holocene, Gulf of California

1. INTRODUCTION

The Gulf of California is a young tectonically opening elongated ocean basin in western Mexico, characterized by a series of central and marginal basins that accumulate thick marine sediment sequences, representing detailed archives for tectonic and paleoclimate reconstructions. The gulf extends across the Tropic of Cancer, spanning the

tropical to temperate climate zones and open in the south to the tropical Pacific Ocean (Fig. 1). Its climatic conditions are controlled by regional seasonal changes of the North American monsoon (NAM), El Niño-Southern Oscillation (ENSO) and migration of the Inter-Tropical Convergence Zone (ITCZ), resulting in contrasting atmospheric and oceanic circulation patterns (*Barron et al., 2005*; *Douglas et al., 2007*; *Pérez-Cruz, 2013*).

Paleoclimatic and paleoceanographic studies have been conducted in the Gulf of California, mainly in sediments from the central and marginal basins (*Donegan and Shrader, 1982*; *Pike and Kemp, 1997*; *Barron et al., 2004, 2005*; *Pérez-Cruz, 2006, 2013*; *Douglas et al., 2007*; *Alvarez et al., 2012*). In contrast, relatively few paleomagnetic and rock magnetic studies had been reported for sediments in the gulf. Recently, rock magnetic studies are being carried out in late Pleistocene and Holocene marine sediments from the southern gulf for paleoclimatic reconstructions and to investigate on sediment sources, terrigenous/biogenic input and depositional processes (*Pérez-Cruz and Urrutia-Fucugauchi, 2010*). Sediments in the central and marginal basins are characterized by

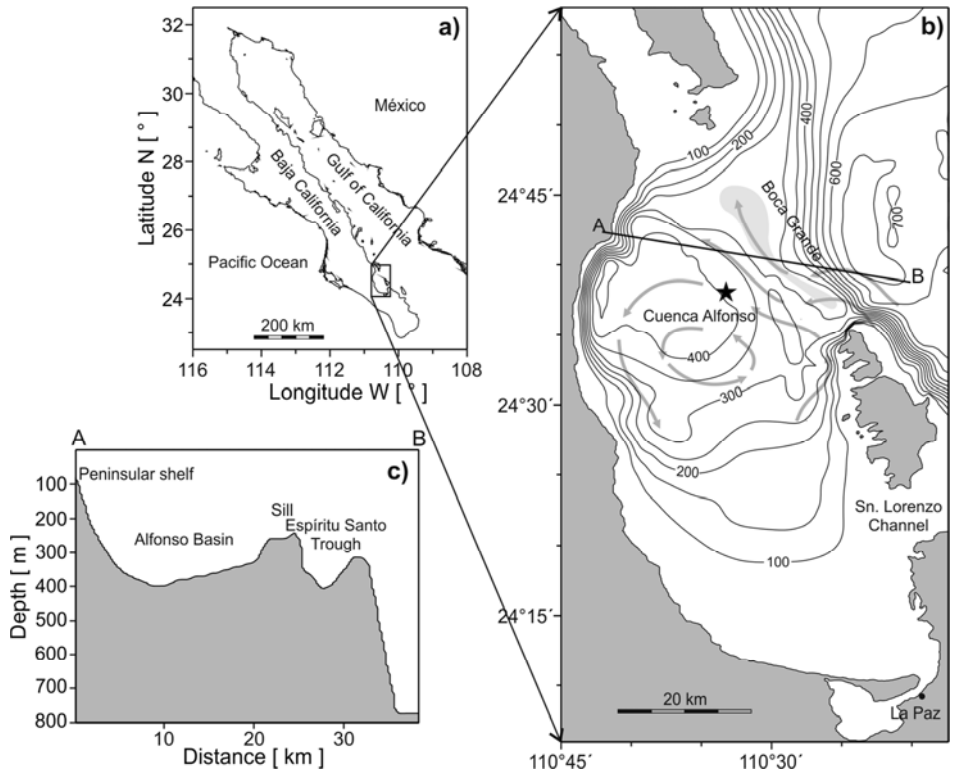

Fig. 1. Location of study area in the Alfonso Basin, southern Gulf of California. **a)** Schematic map of the Gulf of California and western Mexico showing location of the Alfonso Basin. **b)** Bathymetric map of the Alfonso Basin, with drilling site for BAP96-CP core (star in the central basin sector). **c)** Bathymetric cross section from the peninsula margin across the basin, sill and Espiritu Santo trough (*Pérez-Cruz and Urrutia-Fucugauchi, 2010a*).

finely laminated sequences deposited in anoxic conditions, ranging from yearly seasonal to multi-year deposits (*Molina-Cruz et al., 2002*; *Pérez-Cruz, 2013*).

Laminated sediment sequences formed in low oxygen to anoxic environments have been long studied, including the reactions and conditions of early diagenesis (*Berner, 1980*). Diagenetic changes involve a complex array of biochemical reactions, including sulfate reduction, organic matter decomposition and magnetite dissolution (*Berner, 1980*; *Wilson et al., 1985*; *Leslie et al., 1990a,b*; *Verosub and Roberts, 1995*). Evidence on present and past diagenesis is recorded in the iron minerals and in their chemistry, mineralogy and magnetic properties (*Roberts, 2015*). Recently, increased interest in anoxic basins and continental shelves has been driven by induced eutrophication from anthropogenic activities and a warmer ocean (*Helly and Levin, 2004*; *Lyman et al., 2010*; *Hofmann et al., 2011*). Studies have uncovered a broad range of chemical and biological reactions occurring at distinct spatial and temporal scales and the zonations marked by oxidation/reduction conditions (*Froelich et al., 1979*; *Helly and Levin, 2004*; *Canfield and Thamdrup, 2009*).

This study aims to look for and to characterize records of magnetic mineral dissolution zones preserved in marine sediments. Study of diagenetic effects on the magnetic mineralogy of marine sediments is an area of intense research, focusing on oxidation/reduction reactions, magnetite authigenesis, magnetic dilution, magnetization acquisition mechanisms and reliability of paleomagnetic record (e.g., *Karlin, 1990*; *Tarduno, 1995*; *Yamazaki et al., 2003*; *Garming et al., 2005*; *Hayashida et al., 2007*; *Rowan et al., 2009*; *Zheng et al., 2010*; *Roberts, 2015*). The sediments analyzed come from a middle-late Holocene laminated sequence cored in the Alfonso Basin in the southern Gulf of California (Fig. 1b,c). The sequence is finely laminated indicating low oxygen conditions, with the topmost section showing diagenetic effects marked by strong magnetic enhancement factors. Down core magnetic properties are investigated, searching for and identifying past diagenetic effects in the low-oxygen depositional environment.

2. MAGNETIC PROPERTIES AND DIAGENESIS

Rock magnetic properties in sediments have been long investigated, with a wide range of applications in studies of sedimentary processes, basin analysis, sediment sourcing, sea-level variations, and paleoclimatic and paleoenvironmental reconstructions (e.g., *Bloemendal et al., 1992*; *Maher and Thompson, 1999*; *Yamazaki et al., 2003*; *Blanchet et al., 2008*; *Zheng et al., 2010*). The interdisciplinary field of environmental magnetism has rapidly developed with new techniques, instrumentation and applications (*Maher and Thompson, 1999*). Rock magnetic measurements are part of logging techniques in marine sedimentary cores providing initial documentation. Magnetic susceptibility is the most used logging technique for sediment characterization and sequence correlations. Susceptibility core logs, combined with magnetic parameters, granulometry and mineralogical data, provide insight on sediment source, terrigenous input, depositional environment, tephrochronology, and diagenetic and alteration processes. For example, early studies on Late Quaternary sediments from the North Atlantic permitted characterization of glacial sequences associated with high magnetic susceptibility and interglacial sequences with low magnetic susceptibilities (*Robinson et al., 1995*). Climate

variations exert major control on sediment characteristics, including grain sizes, mineralogy, texture, and iron-titanium oxides. Paleoclimatic reconstructions using magnetic parameters have been retrieved from marine sedimentary sequences worldwide.

Magnetic susceptibility is a concentration-dependent parameter, which in sediments characterized by homogeneous magnetite and titanomagnetite assemblages, high and low values indicate high and low magnetic mineral concentrations. This is a useful correlation related to climate, particularly for detrital mineral assemblages where the magnetic susceptibility acts as a paleo-precipitation proxy. There are however several factors affecting the simple correlation, including diagenetic effects resulting in dilution and production of authigenic magnetites. Identification of diagenetic effects becomes more difficult for ancient diagenetic zones which became affected and modified down column (*Brachfeld et al., 2009*; *Rowan et al., 2009*).

Processes acting after sediment burial and compaction overprint and modify the magnetic mineralogy and paleomagnetic record, in the form of secondary magnetizations and new magnetic mineral phases. Diagenetic changes in magnetic mineralogy have been observed in a range of depositional settings and under distinct climatic conditions (e.g., *Karlin and Levi, 1983*; *Karlin, 1990*; *Leslie et al., 1990a,b*; *Tarduno, 1995*; *Yamazaki et al., 2003*; *Garming et al., 2005*; *Hayashida et al., 2007*; *Rowan et al., 2009*; *Brachfeld et al., 2009*; *Kawamura et al., 2012*). *Roberts (2015)* has recently reviewed studies in different environments, from near-shore, tidal, hemi-pelagic and pelagic settings. A variety of redox conditions across offshore-onshore transects, also reflected in organic carbon contents and fluxes, can lead to dissimilar diagenetic transformations.

Magnetic mineral diagenesis occurs in hemipelagic environments in continental margins, in contrast to deep low primary productivity settings. Chemical processes during diagenesis result in acquisition of chemical remanent magnetizations, resetting the paleomagnetic record. Early diagenetic processes alter/generate mineral phases by oxidation and reduction reactions resulting in magnetic mineral dilution and magnetite authigenesis. The magnetic mineral contents decrease depending on various factors, including organic carbon content, sedimentation rate and oxygen conditions. This is reflected in the highly variable depths estimated for the magnetic mineral decrease from a few centimeters to several meters (*Karlin and Levi, 1983, 1985*; *Leslie et al., 1990a,b*; *Kawamura et al., 2008*; *Roberts, 2015*). The diagenetic processes involve a wide range of factors under variable condition, which translates in differences in the chemical and magnetic reactions, magnetic dilution and preservation of the paleomagnetic record.

3. STUDY AREA

The study is conducted in sediments from the Alfonso Basin, at the southwestern sector of the Gulf of California (Fig. 1). Alfonso is a closed marginal small basin with maximum depths of ~420 m, enclosed in the northern sector of Bay of La Paz and separated from the open gulf by an elongated sill. The basin and gulf exchange waters through the northern Boca Grande channel, and through the southern San Lorenzo channel, with Tropical Surface Water flowing to the Bay and increased-salinity Gulf of California Water flowing back to the gulf (*Monreal-Gomez et al., 2001*). Regional climate

is semi-desertic. Evaporation of about 300 mm/yr exceeds precipitation with an average of 180 mm/yr, and rivers discharge is nonexistent.

Pluvial terrigenous and biogenic inputs represent major sources of sediment in Alfonso Basin, with amounts of eolian fine-grained material and the turbiditic currents. Terrigenous sediments in the basin come from local drainages cut in the steep scarps of volcanic tilted blocks in the Baja peninsula within the Comondu silicic tuff sequences. Theyconsist of silicoaluminates derived from the rhyolitic tuffs at the basin western and northern flanks. The low-oxygen conditions in the central sector of the basin allow undisturbed preservation of finely laminated sediments (Fig. 2), representing multiannual laminations (*Molina-Cruz et al., 2002*; *Pérez-Cruz, 2006*).

4. MATERIALS AND METHODS

For the study we selected sediments from a gulf marginal basin where sediments are dominated by detrital material from the surrounding volcanic sequences and biogenic input. Diagenetic effects with oxidation/reduction and magnetite authigenesis might be recorded and possibly preserved down column. The low-oxygen environments allow preservation of fine details. Nevertheless, factors such as wind-blown fine dust with very fine grained magnetic particles and complex assemblages of magnetic minerals might complicate separation of signals in the down core magnetic property logs.

The sediments analyzed come from a Kasten core BAP96-CP recovered at ~390-m water depth in the central sector of the Alfonso Basin at 24°38.12′N, 110°33.24′W. Core is 212 cm long and composed of ~70–90% terrigenous and ~5–7% organic-rich hemipelagic sediments, forming dark and light fine laminations (Fig. 2). Light laminas are formed mainly by biogenic sediments. Chronological control is provided by accelerator mass spectrometry (AMS). AMS dates on benthic foraminifer´s shells indicate that the core spans the past 8000 years BP. Sedimentation rates range from 0.34 mm/yr towards the core top to 0.25 mm/yr below 100 cm, with average whole core rate of 0.39 ± 0.04 mm/yr (*Pérez-Cruz, 2006*). Sequence is characterized by thin turbidites (*González-Yajimovich et al., 2007*; *Pérez-Cruz and Urrutia-Fucugauchi, 2010b*).

The sediment sequence is described from macroscopic observations, X-ray images, microfossils and chemical and physical properties (e.g., *De Diego, 1998*; *Pérez-Cruz, 2006*; *González-Yajimovich et al., 2007*; *Douglas et al., 2007*; *Pérez-Cruz and Urrutia-Fucugauchi, 2010a*). *De Diego (1998)* reported analyses on sediment microfabrics, carbonates, total organic carbon and opal silica, studying the oxygen-related biofacies. In the study she identified five distinct biofacies corresponding to (a) anerobic, (b) quasi-anerobic, (c) exaerobic, (d) dysaerobic, and (e) aerobic, which were interpreted in terms of anoxia and oxygenation alternating events during the late Holocene. Sediment microfabrics correlate with carbonate contents, with increasing carbonates in the laminated sections. Total organic carbon and opal silica on the other hand do not vary with type of biofacies. *De Diego (1998)* proposed that the total organic carbon contents are controlled by dissolution/decomposition rates through the section, with opal silica being also similarly affected.

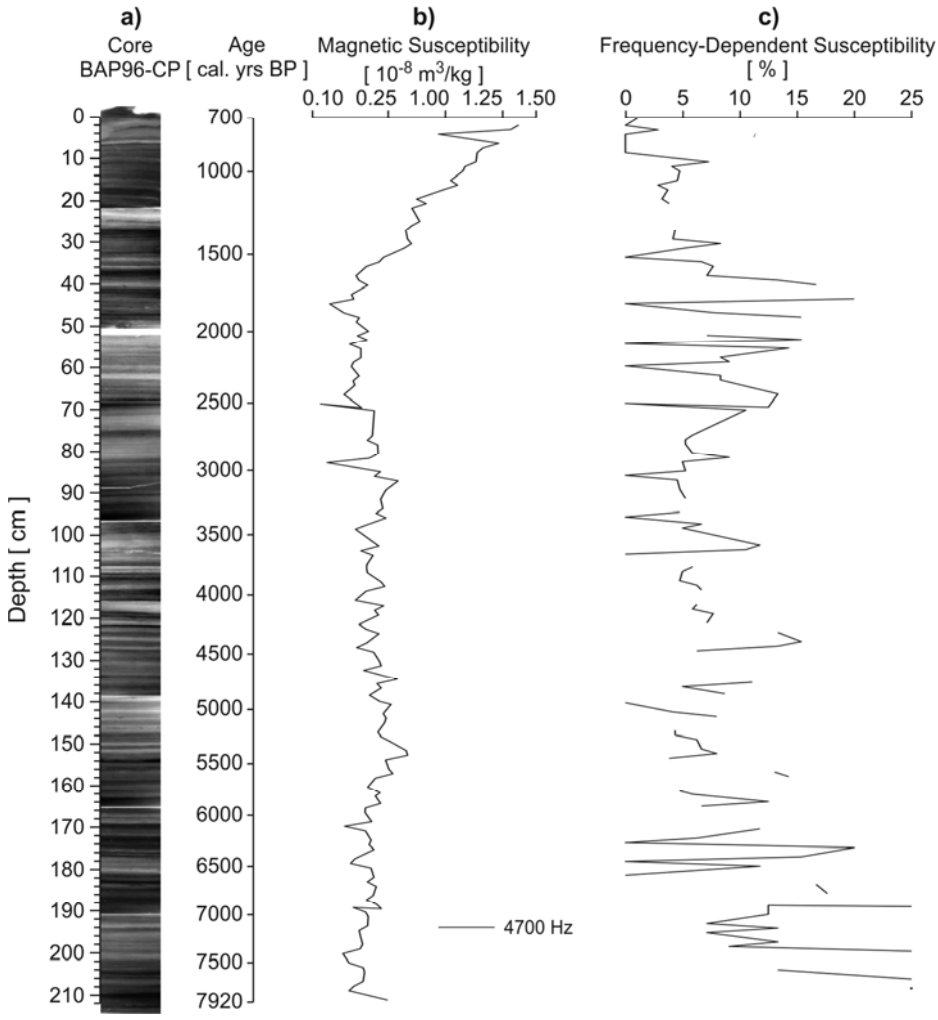

Fig. 2. **a)** X-ray composite images for BAP96-CP core from Alfonso Basin, **b)** magnetic susceptibility, and **c)** frequency-dependent magnetic susceptibility. Data area plotted as a function of core depths and estimated ages from the radiocarbon accelerator mass spectroscopy age model.

5. MAGNETIC PROPERTIES

In the initial study of the Alfonso Basin sediments, the magnetic susceptibility variation down the sediment column was analyzed in terms of variation of terrigenous input, associated with precipitation changes (*Pérez-Cruz and Urrutia-Fucugauchi, 2009*). This is tested by further magnetic measurements of magnetic hysteresis, remanence coercitivity and laboratory remanence imparted magnetizations.

For the study we use magnetic susceptibility, intensity and direction of natural remanent magnetization (*NRM*), micromagnetic hysteresis loops, isothermal remanent magnetization (*IRM*) acquisition and back-field demagnetization of saturation *IRM*, anhysteretic remanent magnetization (*ARM*) acquisition and alternating field (AF) demagnetization of *ARM*. This provides data for characterizing the magnetic mineralogy and properties as applied to the sediment sequence (*Day et al., 1977*; *Dunlop, 2002*). The core was sampled with paleomagnetic 2.2 cm cubic sample holders, from top to bottom with a total of 143 overlapping samples spaced every 1.5 cm. Data on magnetic susceptibility, *NRM* intensity and hysteresis were reported in *Pérez-Cruz and Urrutia-Fucugauchi (2009)*. Here we carried out additional magnetic hysteresis and coercivity measurements, *IRM* and *ARM* acquisition and AF stepwise demagnetization of *NRM*, *IRM* and *ARM*.

Low-field magnetic susceptibility was measured using a Bartington MS2 susceptibility meter equipped with the dual-frequency sensor and analyzed in terms of volume and mass normalized susceptibilities (10^{-6} SI and 10^{-8} m^3/kg, respectively) (*Dearing et al., 1996*). The *NRM* and laboratory-imparted magnetizations were measured with a spinner JR-5 magnetometer. Viscous magnetizations at short- and long-term laboratory storage conditions were monitored, showing no appreciable remagnetization effects (*Urrutia-Fucugauchi, 1981*; *Dunlop, 1983*). The magnetic hysteresis loops, *IRM* acquisition and saturation *IRM* back-field demagnetization were determined on microsamples with the MicroMag system.

Additionally, *IRM* acquisition was imparted in 12 incremental steps up to 1 T using a pulse magnetizer. The *IRM* acquisition curves were analyzed to quantify soft and hard coercivity components using the curve fitting of the acquisition curve as a function of the logarithm of applied field or linear acquisition plot (LAP), the gradient of acquisition plot (GAP) and the standardized acquisition plot on a probabilistic scale (SAP) (*Kruiver et al., 2001*). This analysis of the magnetic coercivity components permits to investigate mixed mineral assemblages, which give rise to cumulative log-Gaussian contributions that are linearly added. The saturation *IRM* was AF demagnetized in 10 steps up to 100 mT. *ARM* was imparted in 14 incremental steps up to maximum alternating field of 100 mT under biasing 0.4 mT direct field with the system. Alternating field demagnetization was carried out in 12 steps up to maximum applied fields of 100 mT using a Molspin AF tumbling demagnetizer.

6. RESULTS

The low-field magnetic susceptibility log shows high values in the upper section followed by low amplitude low frequency fluctuations down core. Susceptibility varies from about 0.5 to 8.8–9.0 × 10^{-6} SI, with values up to 4 times higher in the top sediments followed by low values around 1.5–3 × 10^{-6} SI (Fig. 2). The corresponding mass-specific susceptibilities at low and high frequencies vary between 0.1 and 1.4 × 10^{-8} m^3 kg^{-1}. The magnetic susceptibility was re-measured at distinct times to evaluate instrumental noise effects and the reproducibility of the logs. The results showed no noise effects affecting the measurements at low and high frequencies, which could result in noisy frequency-dependent susceptibility. This procedure also permits assessing "storage" diagenetic

effects, which result in decrease of remanence intensity and susceptibility (*Richter et al., 1999*) and acquisition of secondary viscous remanence components (*Urrutia-Fucugauchi, 1981*; *Dunlop, 1983*). The variation pattern with depth is characteristic of changes in concentration of magnetic minerals through the laminated sequence andcorrelation with the X-ray images and lithological column points to variations in terrigenous input. Frequency-dependent susceptibility fluctuates from fluctuate up to ~25 %, with a tendency to increase towards the bottom of the core. The frequency-dependent susceptibility displays a marked change at about the middle to late Holocene transition, with high more variable values in the middle Holocene than during the late Holocene.

In Fig. 3 the logs of magnetic susceptibility, density, total organic carbon, remanent and saturation magnetization intensities are compared. The magnetic susceptibility, *NRM* and saturation magnetization intensities show high values in the top sediments decreasing to lower values down core, with maxima at ~90 and ~150 cm depth correlating with the density variation. The susceptibility maxima suggest higher relative contents of titanomagnetite minerals. Intensity of remanent magnetization shows a pattern with higher values in the top sediments and relatively smooth changes with depth. *NRM* intensity varies between about 1 and 2 mA/m, with values in the top surface sediments up to 8 mA/m. The variation in sediment density inversely correlates with the total organic carbon contents (*De Diego, 1998*), with a minimum between about 125 and 170 cm corresponding to highs in the density and susceptibility logs. From 140 to 160 cm there is an apparent increase in terrigenous input, marked by the increase in density, decrease in organic carbon and slight increase in magnetic susceptibility. This could reflect coarser grain sizes, although there is no noticeable change in the remanence and saturation intensities.

Magnetic hysteresis loops indicate saturation at low fields, suggesting titanomagnetites and magnetite with restricted grain size ranges (Fig. 4a). Hysteresis loops are dominated by paramagnetic components whose relative contributions vary with depth. Intensity of remanent (M_{rs}) and saturation (M_s) magnetizations is highest in the surface sediments. The paramagnetic slope correction parameter shows higher values in the shallow sediments down to 30–40 cm depth followed by cyclic variation down core. After slope correction, loops show saturation at low fields with high saturation magnetization values, characteristic of low-tititanomagnetites and magnetite. Plots of hysteresis magnetization and coercivity ratios (*Day et al., 1977*; *Dunlop, 2002*) show that samples fall in the pseudo-single domain (PSD) field (Fig. 4b). The dominant magnetic minerals are low coercivity fine-grained titanomagnetites and magnetite with PSD behavior, which may represent mixtures of single domain (SD) and multidomain (MD) particles.

Contribution of superparamagnetic (SP) fine-grained (< 50 nm) particles is higher at some intervals, which is recorded in the hysteresis parameter ratio plots and the frequency-dependent susceptibility (*Dearing et al., 1996*; *Dunlop, 2002*; *Rowan et al., 2009*). Analysis of the field dependence effects indicate that varying field strengths can affect the frequency-dependent measurements (*Jackson et al., 1998*). Additional measurements to identify presence of SP particles using magnetic hysteresis and anhysteretic remanence acquisition and AF demagnetization are used. Superparamagnetic SP particles are indicated in the magnetic domain plot, with hysteresis ratio values being

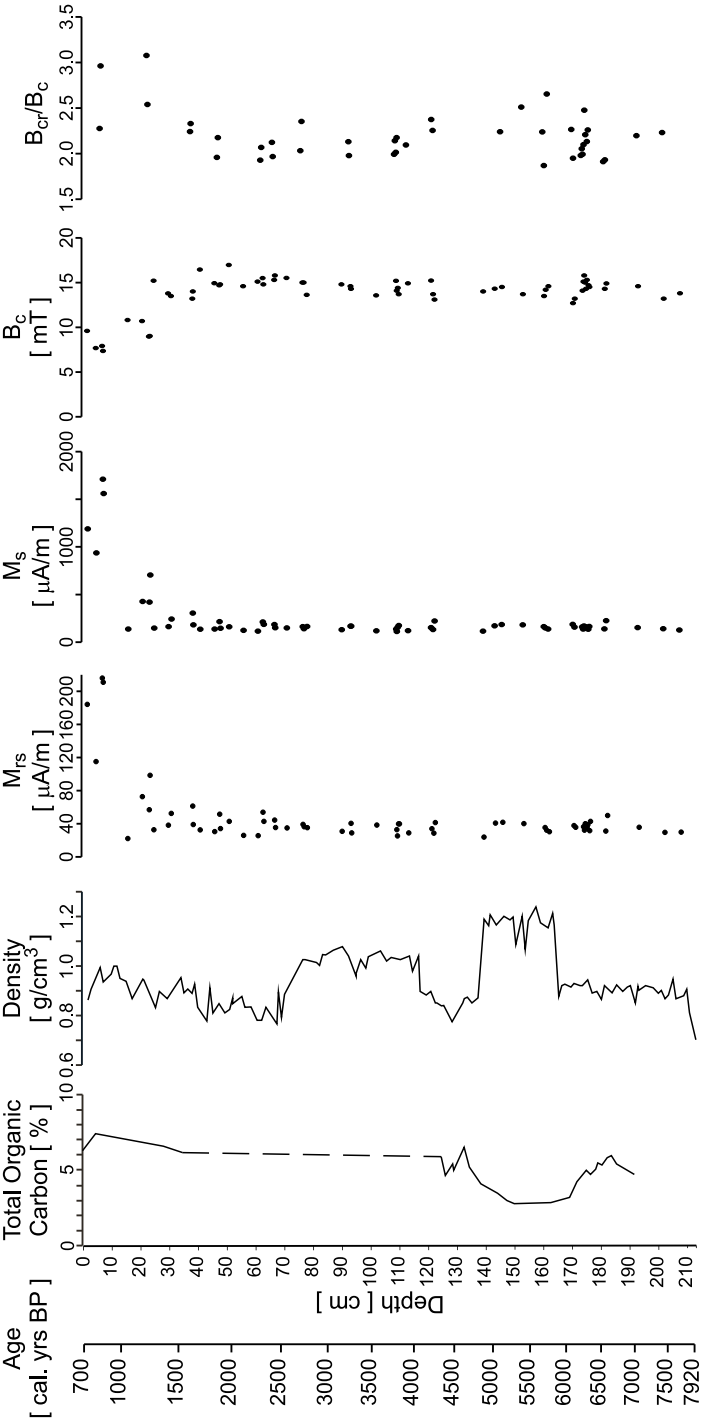

Fig. 3. **a)** Total organic carbon (*De Diego, 1998*); **b)** density; **c)** remanent magnetization M_{rs}; **d)** saturation magnetization M_s; **e)** coercive force B_c; and **f)** ratio of coercivity of remanence B_{cr} and coercive force B_c (*Pérez-Cruz and Urrutia-Fucugauchi, 2009*) as a function of depth and age.

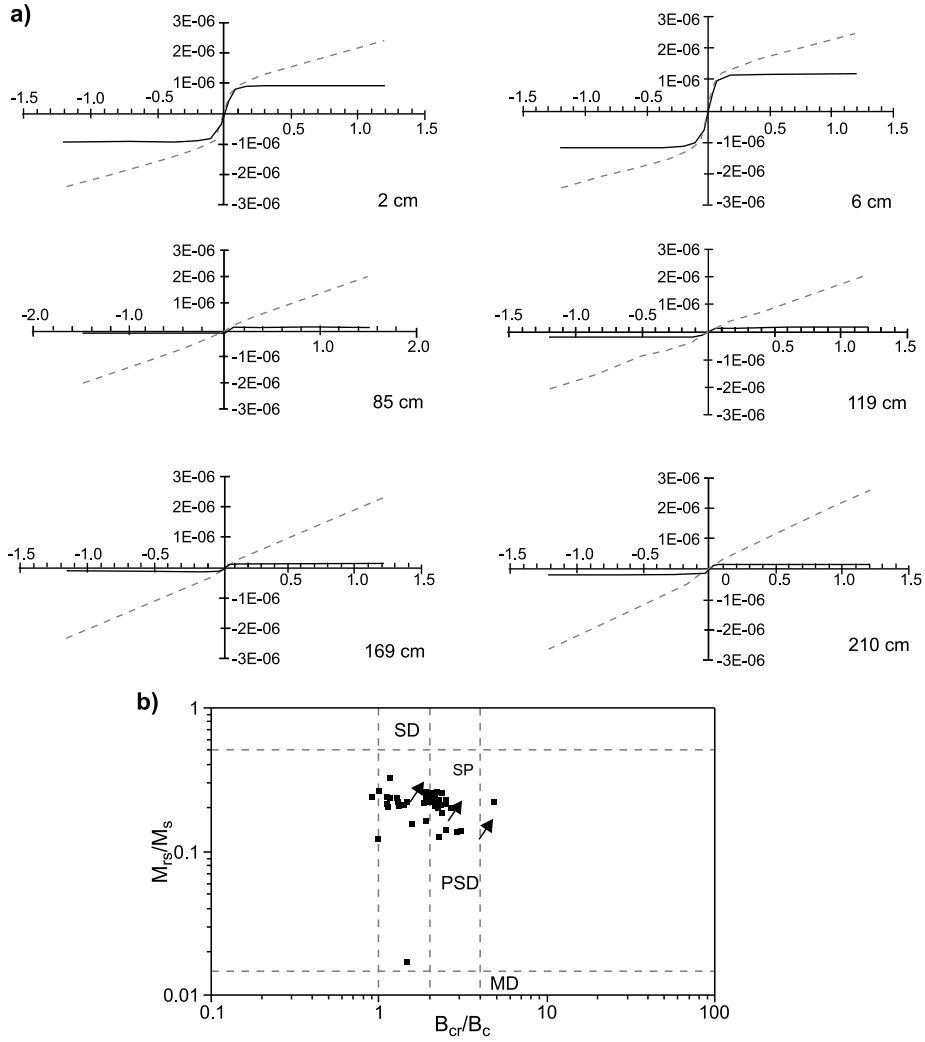

Fig. 4. **a)** Magnetic hysteresis loops for samples from different depths along the core before and after the correction for paramagnetic slope (grey dashed and full black curves, respectively). Note that the relative contents of ferrimagnetic minerals decreases down core, correlating with the magnetic susceptibility logs and other rock magnetic data. **b)** Plot of magnetic ratios of domain state for the BAP96-CP core (data from *Pérez-Cruz and Urrutia-Fucugauchi, 2009*, and this study). Most samples plot in the pseudo-single domain (PSD) field, representing a mixture of single domain (SD) and multidomain (MD) particles. Arrows indicate apparent displacement from the mixing SD-MD trends to the superparamagnetic (SP) field (*Dunlop, 2002*).

displaced upwards in the PSD domain field (*Dunlop, 2002*). The SP very fine-grained fraction does not carry a remanence at room temperature. The frequency-dependent susceptibility varies with depth and shows a variation pattern with higher values in the bottom section that correlates with the susceptibility log.

The *ARM* acquisition curves and AF demagnetization of *ARM* acquired at 100 mT are similar through the core (Fig. 5), indicating an assemblage of low coercivity magnetites and titanomagnetites. Plot of the *ARM* intensity as a function of magnetic susceptibility shows a cluster at low values and a linear correlation, except for the uppermost sediments (Fig. 6), suggesting similar grain size distribution with varying concentrations of titanomagnetites and magnetite trough the core. A common grain size distribution with changing concentration is consistent with the similar hysteresis loops. After slope correction loops are similar through the section, with saturation at low fields indicative of magnetites and titanomagnetites. Hysteresis loops indicate variable amounts of paramagnetic minerals. In the hysteresis parameter ratio plot, samples fall in the PSD domain field (Fig. 4).

IRM acquisition curves are characterized by rapid increase in field less than 100 mT, indicating low coercivity minerals, compatible with magnetite and titanomagnetites

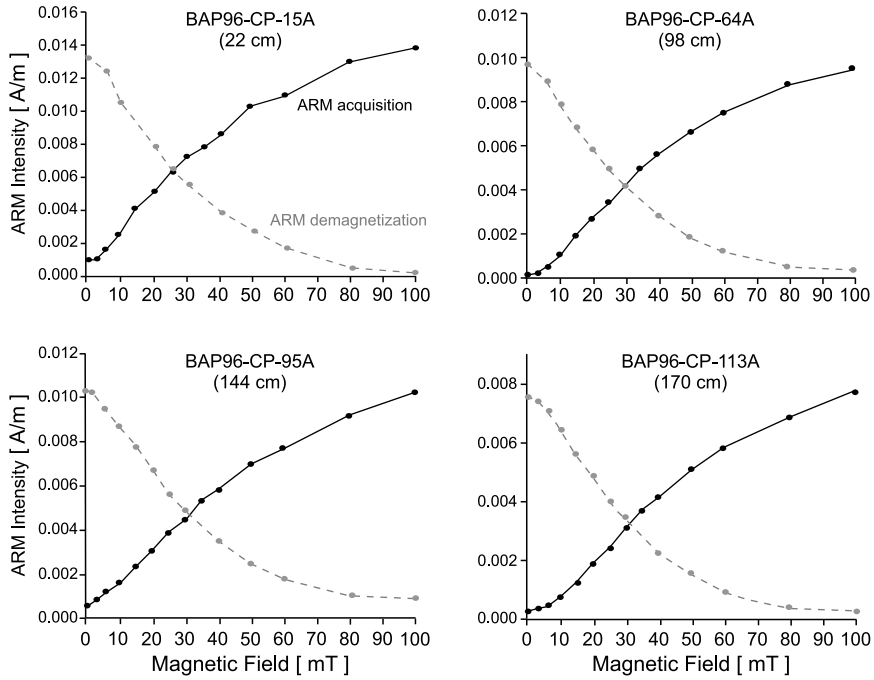

Fig. 5. Plots of anhysteretic remanent magnetization (*ARM*) acquisition curves and alternating field (AF) demagnetization of *ARM* acquired at 100 mT fields. The *ARM* acquisition and AF demagnetization curves are similar through the core, indicating presence of a magnetite and titanomagnetite assemblage. Median destructive fields are around 20 mT. The intersection AF field between *ARM* acquisition and AF demagnetization curves ranges from 20 to 30 mT.

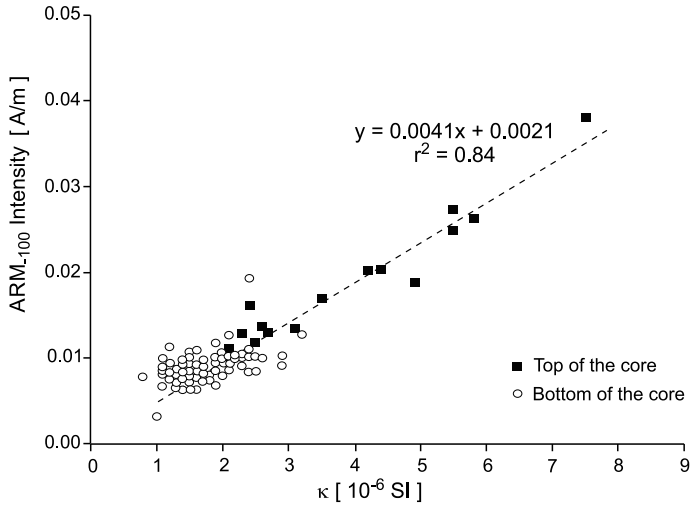

Fig. 6. Anhysteretic remanent magnetization (*ARM*) intensity plotted as a function of low-field magnetic susceptibility (κ).The regression line and regression fit coefficient r^2 are calculated for all samples plotted in the diagram, note that the three topmost samples with highest magnetic susceptibility are not included. In the diagram, the samples in the top section of the core show a larger range in *ARM* intensity and susceptibility as compared to the sections down core; they are indicated in red squares.

(Fig. 7a). Curves show a tendency to saturate in 800–1000 mT applied fields, but without reaching saturation. This suggests varying contributions of high coercivity minerals. The *IRM* intensities acquired at 1 T fields show higher values in the upper surficial sediments with lower values down the section (Fig. 8a). The pattern correlates with the other magnetic logs showing higher concentration of magnetic minerals and the dissolution effects with depth. The rate of change through the section is estimated with the horizontal gradient of the *IRM* intensity log (Fig. 8b), which separate the upper section and the zones with higher rate change. Non-saturating *IRM* acquisition curves characterize assemblages with different coercivities, which for instance is the case for mixtures of titanomagnetites and magnetite with greigite, hematites or goethite. Application of the cumulative log-Gaussian analysis of *Kruiver et al. (2001)* using the linear acquisition plot, the gradient acquisition plot and the standardized acquisition plot indicates small high coercivity components. The linear acquisition plot (LAP), gradient acquisition curve (GAP) and standardized acquisition plot (SAP) curves are similar through the section (Fig. 9), suggesting a homogeneous mineral assemblage with varying contents of magnetic minerals. The higher contents of magnetite in the surficial sediments are reflected in the steeper slop in the LAP curve and the LAP and SAP curve shapes (Fig. 9). The maximum *IRM* was AF demagnetized (Fig. 7a). Median destructive fields vary from 20 to 32 mT, with a remanence fraction of 10–20% remaining after AF demagnetization to 100 mT. *IRM* acquisition and AF demagnetization curves are similar through the sediment section, with high intensity values in the upper section.

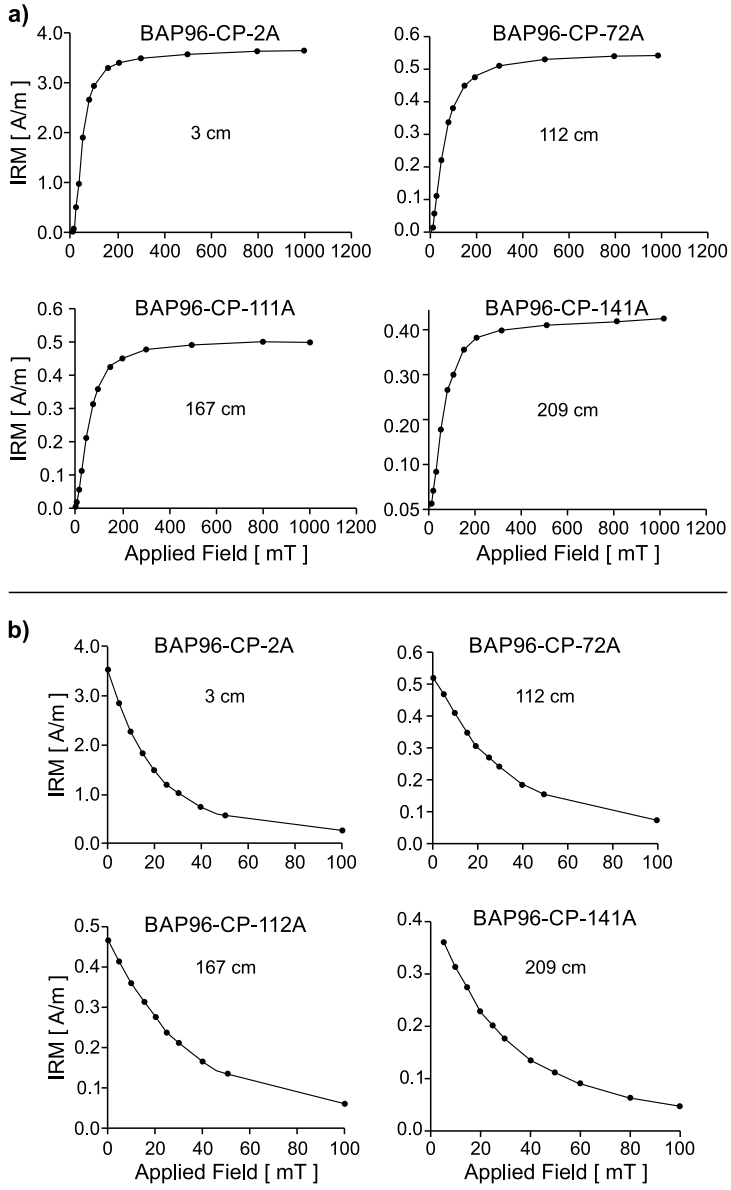

Fig. 7. Plots of **a)** isothermal remanent magnetization (*IRM*) acquisition and **b)** alternating field demagnetization of saturation *IRM*. Saturation *IRM* intensities are higher in the upper core section. Median destructive fields are around 20 to 32 mT.

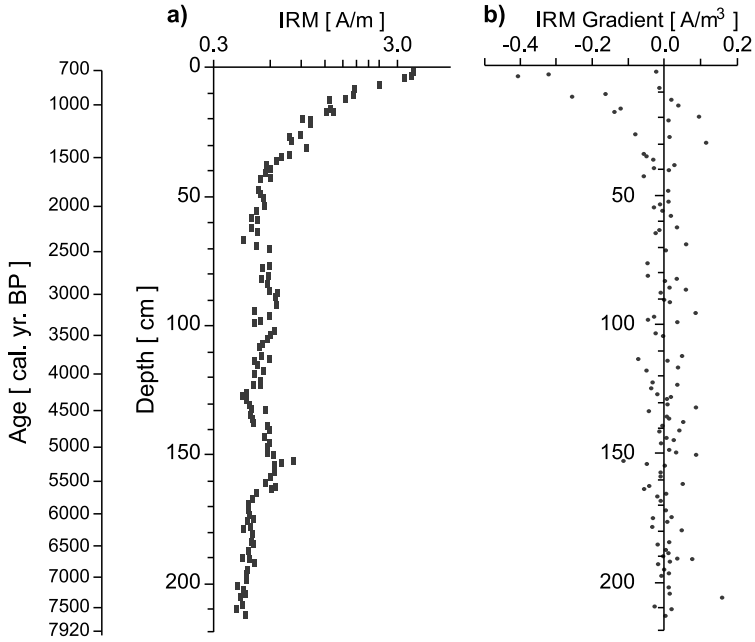

Fig. 8. **a)** Saturation (or maximum) *IRM*, and **b)** gradient of saturation *IRM* as a function of age and depth.

7. DISCUSSION

Since the early studies on diagenetic effects on the magnetic properties of marine sediments, it was proposed that iron oxides are progressively reduced, sulfidized and pyritized with decomposition of organic matter (*Karlin and Levi, 1983*; *Karlin, 1990*; *Leslie et al., 1990a,b*). Magnetic assemblages in surface sediments with detrital magnetites undergo dissolution, with sediments characterized by higher values of natural remanent and laboratory-induced magnetization intensities at the top and significantly lower values at depth. Selective dissolution of the fine-grained minerals results in down-section coarsening of the magnetic fraction, with iron reduction taking place before sulfide formation. The magnetic mineralogy and mineral reactions involving SP sulfide particle enrichment related to the sulfate/methane transition migration have been investigated and modeled (*Rowan et al., 2007*). Other studies have documented down core enrichments in SD and SP particles due to progressive dissolution in MD and PSD particle surfaces (*Karlin and Levi, 1985*).

Studies on sediments from a wide range of depositional settings have documented characteristic variation patterns, related to reductive diagenesis producing a reduction in magnetization intensity, coarse magnetic grain sizes and new magnetic phases. In oxygen-depleted settings with high sedimentation rates, detrital magnetite and titanomagnetites are affected by dissolution during diagenesis (*Richter et al., 1999*; *Passier et al., 2001*;

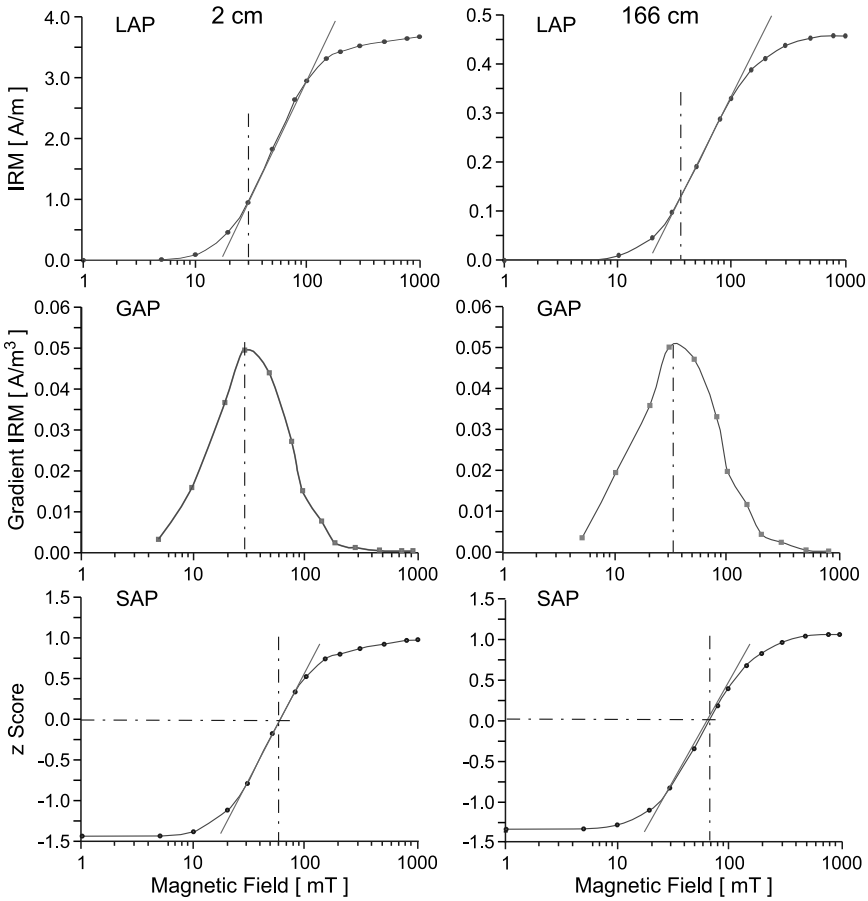

Fig. 9. Cumulative log-Gaussian analysis of the isothermal remanent magnetization (*IRM*) acquisition curves, with the linear acquisition plot (LAP), gradient acquisition curve (GAP) and standardized acquisition plot (SAP) for samples from the surficial section (2 cm) and deeper section (166 cm). The sample from the surficial section in the magnetite dissolution zone is characterized by high *IRM* intensities, while the sample from the lower section is characterized by weaker *IRM* intensities.

Yamazaki et al., 2003; *Brachfeld et al., 2009*; *Rowan et al., 2009*). *Leslie et al. (1990a,b)* estimated that up to 90% of the magnetite contents in surficial sediments from the California Borderland San Pedro, Santa Catalina and San Nicolas basins gets dissolved at depth in the sediment column. The magnetite dissolution is marked by 1 to 2 orders of magnitude decrease in magnetic susceptibility and remanence intensity. They used chemical, magnetic and X-ray diffraction to constrain the mineralogy and mineral reactions during diagenesis in the anoxic sediments. From the sulfate reduction rates and ferric oxyhydroxide fluxes, the dissolution onset depths were estimated to range between

5 and 40 cm depth. *Leslie et al. (1990a,b)* reported changes in the coercivity in the surficial sediments from soft to hard coercivities. *Karlin (1990)* reported formation of authigenic magnetites with oxidative decomposition of organic matter occurring above the iron reduction zone. *Hayashida et al. (2007)* studied the diagenetic effects on sediments from the Japan Sea using magnetic concentration parameters such as magnetic susceptibility, *ARM* and *IRM* magnetizations, with higher values in top sediments by one or two orders of magnitude, and loss of fine-gained magnetite taking place between 1.2 to 0.6 m below the surface.

In the BAP96-CP core, magnetic concentration parameters show higher values in the top, with values decreasing down core, consistent with selective dissolution of fine-grained iron oxides resulting in decrease of magnetization intensity, coarse magnetic grain sizes and low susceptibilities. The selective dissolution is observed in the stratigraphic variation in susceptibility, hysteresis parameters and laboratory-induced *IRM* and *ARM* remanences. Magnetic minerals in the sediments include magnetite, low-titanium titanomagnetites and iron sulfides, with relatively constant low to intermediate coercivity magnetite and titanomagnetites of detrital origin from the volcanic tuff sequences surrounding the basin.

The variation with depth in susceptibility and magnetization logs records diagenetic changes with formation of authigenic magnetites by oxidative decomposition of organic matter during dewatering and compaction occurring above the iron reduction zone. Upon burial, the fine-grained fraction is affected by dissolution within the zone of iron reduction. Changes in non-steady state redox conditions associated with variations in primary productivity and depositional rates of biogenic and terrestrial sediments due to climatic and oceanographic factors affect dissolution processes. *Rowan et al. (2009)* proposed that progressive dissolution of SD and PSD magnetite with formation of SD/SP greigite at the sulfate/methane transition (SMT) zone modifies the magnetic mineral distribution with depth. The initial magnetite assemblage at the surface sediments with a range of domain states and grain sizes is affected by dissolution with migration of the SMT zone. With increasing depth, sediments show small magnetic mineral contents, with low susceptibilities and remanent intensities. Diagenetic enhancement of SP particles (*Tarduno, 1995*) and SD grains increases at depth.

In the study by *Rowan et al. (2009)* results for sediment cores from the northern California and the Oman margins were analyzed. Four intervals with distinct magnetic behaviors were identified, corresponding to the model zones with (zone 1) the primary magnetic assemblage of SD/PSD/MD magnetite, (zone 2a) recent dissolution front, (zone 2b) mildly altered magnetic assemblage separated by an old dissolution front and (zone 3) zone of increasing SD greigite with extended growth (Fig. 10a). The magnetic property logs for the northern California and Oman margins recorded the down core variations resulting from diagenesis with the Oman sediments better recording the recent and old dissolution fronts. The magnetic susceptibility did not show high values in the top sediments, increasing towards the base in zone 1. Zone 3 was characterized by low susceptibility, *NRM*, *IRM* and *ARM* intensities. In the Oman sediments zone 3 showed a trend to higher values in the *S*-ratio and ARM/IRM ratio.

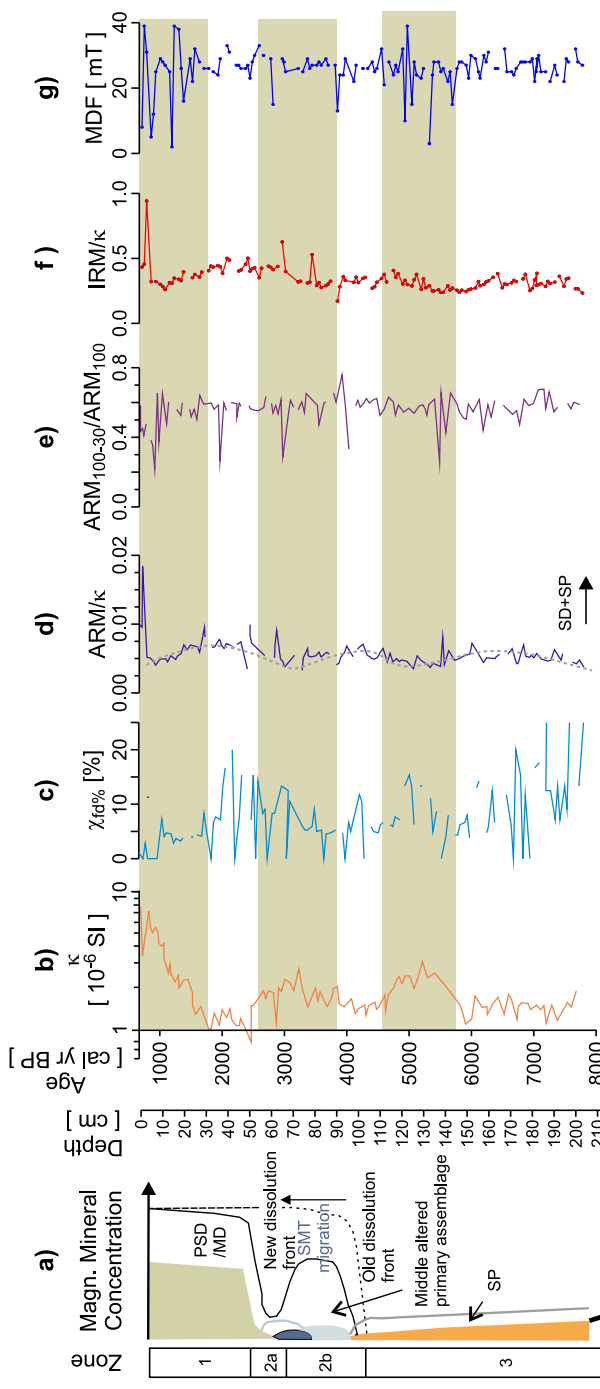

Fig. 10. Magnetic property logs and model of magnetic mineral diagenesis. **a)** Model of magnetic mineral diagenesis (*Rowan et al. 2009*) with simplified down core changes in magnetic mineral content with progressive dissolution of SD and PSD magnetite (dark grey area/line) and formation of SP/SD greigite (light grey line/area) at the sulfate-methane transition (SMT). Note the down core variations with the recent and old dissolution fronts. Model shows recent SMT upward migration and preservation of enriched PSD/MD magnetitein between the dissolution fronts. **b)** Magnetic susceptibility κ. **c)** Frequency-dependent susceptibility $\chi_{fd\%}$. **d)** Anhysteretic remanent magnetization (*ARM*) imparted at 100 mT field normalized by κ. **e)** *ARM* ratio determined as difference between *ARM* imparted at 30 and 100 mT fields normalized to *ARM* at 100 mT. **f)** Isothermal remanent magnetization (*IRM*) acquired at 1.5 T normalized by κ. **g)** Median destructive field (*MDF*) along core (alternating magnetic field required to demagnetize 50% of the saturation remanent magnetization). Note the correlation among the magnetic mineral domain states/grain size and concentration parameters. Magnetic mineral dissolution zones are indicated by the minima in the magnetic susceptibility and the maxima in the *ARM*/κ logs. Recent and old dissolution fronts are preserved down core marking the diagenetically altered magnetic mineral assemblages.

Magnetic properties are here examined in terms of early diagenetic effects (*Rowan et al., 2009*), using the magnetic susceptibility as proxy for magnetic mineral concentration and the frequency-dependent susceptibility and *ARM* as proxies for SP-SD particles (*Dearing et al., 1996*; *Worm, 1998*). The down core pattern correlates with the model expected fluctuations associated with the diagenetic changes, showing the recent and old dissolution fronts (Fig. 10a). The magnetic susceptibility, the frequency-dependent susceptibility, the normalized IRM/κ, the ARM_{100-30}/ARM_{100}, the normalized $SIRM/\kappa$ and the median destructive field *MDF* are plot in Fig. 10 for correlation of proxies on magnetic mineral concentration and dominant domain state mineral particles trough the sediment column. Magnetic property logs show a reduction of magnetic minerals with depth (Fig. 10) and characteristic trends which are interpreted as past dissolution fronts and diagenetically altered zones.

The susceptibility, hysteresis and magnetization logs show high values in the surface sediments and a pattern of variations of low amplitude (Figs 2, 3, 8 and 10). The mass-specific magnetic susceptibility shows an order of magnitude decrease from the surface values to a depth of around 30 cm down core (Fig. 10b). The variation in magnetic mineral concentration and distribution of SD, MD and SP particles record preservation of recent and old dissolution fronts resulting from upward migration of the sulfate-methane transition and preservation of enriched PSD/MD magnetite in between the dissolution fronts (*Rowan et al., 2009*). Three dissolution fronts are identified characterized by susceptibility minima, higher amplitude variable frequency-dependent susceptibility and high ARM/κ (Fig. 10).

The frequency-dependent susceptibility shows intervals with higher and lower variability through the core. Intervals with high susceptibility correspond to small frequency-dependent susceptibility, whereas intervals of low susceptibility show variable (high and low) values (Fig. 10c) of frequency-dependent susceptibility. The frequency-dependent susceptibility values versus depth suggest increasing contents of SP particles, with an assemblage of SP and SD particles in the bottom section. The progressive greigite formation was interpreted from the changes in the hysteresis magnetization and coercivity ratios, with higher B_{cr}/B_c ratios in zone 2, marked by trends looping (*Rowan et al., 2009*; *Roberts, 2015*). In the hysteresis ratio plot for the Alfonso sediments, we do not observe the looping and trend to higher B_{cr}/B_c ratios. The data point distribution shows effects of SP particles (Fig. 4b). Higher resolution with closely spaced samples is needed to evaluate the trends in the magnetization and coercivity ratios. Presence of greigite on continental margin hemi-pelagic settings has not been easy to confirm, requiring detailed rock magnetic property analyses (*Roberts, 2015*; *Roberts et al., 2011*). Further work is needed to identify and quantify the iron sulfide minerals.

Relative contents of fine grained magnetic particles are evaluated using *ARM* acquisition curves and AF demagnetization of *ARM* imparted at 100 mT AF field. In Fig. 6d the *ARM* intensity (sensitive to grain size and concentration) normalized by the low-field susceptibility (sensitive to concentration) is used to evaluate presence of SP and SD particles. The ARM_{100}/κ log correlates with the frequency-dependent susceptibility and it is inversely correlated to the magnetic susceptibility (Fig. 10b,c,d). Intervals with

low susceptibility values are characterized with higher values of the frequency-dependent susceptibility and ARM_{100}/κ.

To evaluate the *ARM* coercivity spectra, we compared the median destructive field (field applied to reduce the *ARM* intensity by 50%), the intersection field between the *ARM* acquisition and the AF demagnetized curves and the ratio of the difference between *ARM* acquired at 30 and 100 mT normalized by the *ARM* at 100 mT. The ARM_{100-30}/ARM_{100} normalized ratio fluctuates around 0.58 through the core, with some samples around 0.28 and others with lower values (Fig. 10e). The similar coercivity spectra of ARM support homogeneous magnetic mineral assemblage through the sequence. The samples with saturation at low fields are spaced through the section and might correlate with input of detrital magnetite and titanomagnetites. They appear regularly spaced and will be interesting to investigate them further. Some of these intervals correlate with thin turbiditic layers (*Gonzalez-Yajimovitch et al., 2007*; *Pérez-Cruz and Urrutia-Fucugauchi, 2010b*); sampling resolution with measurements in the $2.2 \times 2.2 \times 2.2$ cm cubes, however, does not allow detailed correlation.

The normalized *ARM* and *IRM* intensity logs show low amplitude sinusoidal trends that inversely correlate with the magnetic susceptibility log (Fig. 10d,f). The coercivity also shows a characteristic pattern. In Fig. 10g, coercivity is estimated in terms of the median destructive field *MDF*. In the upper sediments *MDF* varies from low to high values up to 40 mT, followed by relatively few changes around 25 mT down core. The dissolution zones marked by higher magnetic susceptibility values show higher variability from soft to hard coercivities (Fig. 10g). This could be possibly associated with partial dissolution of fine grained magnetites accompanied with decrease in *NRM*, *IRM* and *ARM* intensity.

The formation and preservation of the laminae relate to the anoxic conditions, deposition rates and variations in biogenic productivity and terrestrial input. Analysis of the magnetic property variations in individual lamina provides further insight on the diagenetic processes, supporting that fine grained magnetites can be affected by dissolution under anoxic conditions (*Kawamura et al., 2008*). The oxidation/reduction effects produce variation patterns in apparent homogeneous sediments (*Kawamura et al., 2008*) such as in finely laminated sequences (e.g., Fig. 2). *Pérez-Cruz and Urrutia-Fucugauchi (2010a)* reported results of geochemical and magnetic hysteresis data for 41 dark and light laminae, which are used to document variation patterns trough the section. The remanent and saturation magnetizations plotted as a function of relative position (Fig. 3a,b) show higher values in the topmost sediments and lower values through the section. Magnetic coercivity is slightly lower between 6 and 11 mT in the topmost sediments and increases for the rest of the section with mean values varying between 13 and 15 mT, suggesting grain-size changes. The magnetic hysteresis parameters show similar patterns than the other magnetic concentration data, showing a small amplitude low frequency variation. Considering that light and dark laminae indicate higher biogenic or terrestrial input, respectively (e.g., *Donegan and Shrader, 1982*; *Pike and Kemp, 1997*), it is interesting to examine if high hysteresis magnetization intensities correlate with the dark laminations. High magnetizations in dark laminae are associated with preferential dissolution during diagenesis. The plots however do not support a correlation, with higher and lower values in dark and light laminae. The mixed pattern can be due to diagenetic

changes as suggested by *Vigliotti (1997)* for laminated sediments from the Japan Sea. *Vigliotti (1997)* reported higher magnetic concentrations of fine-grained minerals in the light layers as compared to the dark layers, which was related to magnetite dissolution affecting the dark layers. To further analyze the apparent low amplitude variations, polynomial fits were added to the data, which delineate alternating zones of high and low magnetization intensities in dark and light layers (*Pérez-Cruz and Urrutia-Fucugauchi, 2010a*).

Magnetic susceptibility in marine sediments is increasingly used for paleoceanographic and paleoclimate reconstructions and there is a strong interest in further understanding the depositional and post-depositional effects on the magnetic signal (*Verosub and Roberts, 1995*; *Dinares-Turell et al., 2003*). The relationships or dependence of climate and environmental records, diagenesis and the paleomagnetic signal are being investigated, assessing diagenetic processes and smoothing/modification effects (e.g., *Vigliotti, 1997*; *Hounslow and Maher, 1999*; *Yamazaki et al., 2003*; *Brachfeld et al., 2009*; *Zheng et al., 2010*; *Kawamura et al., 2012*). Separation of detrital, diagenetic and biogenic inputs remains a difficult problem in the analysis of sedimentary sections. Biogenic magnetite synthesized by magnetotactic bacteria has been better documented. In contrast preserved biogenic greigite has been more difficult to isolate. Occurrence of diagenetic greigite has been related to climate and terrigenous input variations, with greigite formed in high-humidity warm conditions (*Chang et al., 2014*).

Magnetic mineral dissolution processes have been shown to be related to depositional and climatic conditions (e.g., *Viglioti, 1997*; *Hounslow and Maher, 1999*; *Zheng et al., 2010*; *Roberts, 2015*). The magnetic susceptibility is less modified by magnetic mineral dissolution in contrast to the remanence intensity. Magnetic susceptibility reflects variations in the coarse silt fraction. The variations in grain size could in turn be climatically controlled, reflecting changes in precipitation and sediment runoff into the basin. The implications for climatic and depositional changes are not here discussed, with the relationships requiring further analysis. In the Alfonso sediment sequence, correlation of the magnetic susceptibility logs and the density and total organic carbon records suggests that the small amplitude low frequency variations recorded in the magnetic parameters relate to climatic changes. Total organic carbon shows a broad inverse correlation with magnetic susceptibility and density; though additional *TOC* data are needed to test the relationships (Fig. 3). The apparent periodicities in the susceptibility and magnetic property records of roughly 1200–1500 years correlate with regional climatic signals recorded in North America (*Pérez-Cruz, 2006*; *Viau et al., 2002*; *Miao et al., 2007*). Climate changes in precipitation and ocean temperature relate to regional seasonal variability of the North American monsoon and to ENSO events and mean ITCZ latitudinal migration, which are recorded in the detrital-biogenic input to the basin (*Barron et al., 2004, 2013*; *Pérez-Cruz, 2013*; *González-Yajimovich et al., 2005*; *Douglas et al., 2007*; *Alvarez et al., 2012*).

8. CONCLUSIONS

Magnetic susceptibility log for the marine sediments in the Alfonso Basin in the southern Gulf of California, shows a characteristic pattern with high values at the top

decreasing down core, which record recent and past diagenetic effects. The high values at the surface sediments decrease exponentially in the upper sediments, followed by low amplitude variations with depth. Rock magnetic analyses suggest that the sharp reduction in magnetic mineral contents results from diagenetic processes, modifying the magnetic signal through the sediment column. Changes in magnetic properties along the sediment core show high relative concentrations of magnetite in the shallow sediments decreasing with depth, recording the diagenetic effects resulting from dewatering, compaction and decomposition of organic matter in the laminated sediments. The magnetic susceptibility log shows high values at the topmost sediments followed by small amplitude low frequency fluctuations, which correlate with magnetic concentration parameters of natural remanent and anhysteretic remanence intensity, saturation isothermal remanent intensity and coercivity parameters. Enhancing of magnetic susceptibility up to four times in the upper sediment zone results from formation of authigenic magnetites and marked by increase of magnetization intensities and magnetic stability parameters. The magnetic logs record preservation of old and recent dissolution fronts resulting from enriched pseudo-single domain to multidomain PSD/MD magnetites in between the dissolution fronts.

Acknowledgments: This study forms part of the PALEOMAR Project on the Gulf of California. Critical review comments on the paper by Editor Claudia Gogorza, Konstantin Choumiline and three anonymous journal reviewers have been useful in improving the manuscript and are gratefully acknowledged. We thank Victor Macias, Miguel Diaz and Martin Espinosa for technical assistance in the laboratory. Partial support from the UNAM CABO DIPAL oceanographic cruises and the PAPIIT IN-101012 and IG-111115 and Conacyt infrastructure grant is acknowledged.

References

Alvarez M.C., Pérez-Cruz L. and Hernández-Contreras R., 2012. Coccolithophore and silicoflagellate records in Middle-Late Holocene sediments from La Paz Basin (Gulf of California): Paleoclimatic implications. *Stratigraphy*, **9**, 169–181.

Barron J.A., Bukry D. and Bischoff J.L., 2004. High resolution paleoceanography of the Guaymas Basin, Gulf of California during the past 15,000 years. *Mar. Micropalentol.*, **50**, 185–207.

Barron J.A., Bukry D. and Dean W.E., 2005. Paleoceanographic history of the Guaymas basin, Gulf of California, during the past 15,000 years based on diatoms, silicoflagellates, and biogenic sediments. *Mar. Micropaleontol*., **56**, 81–102.

Berner R.A., 1980. *Early Diagenesis*. Princeton University Press, Princeton, NJ.

Blanchet C.L., Thouveney N. and Vidal L., 2009. Formation and preservation of greigite (Fe_3S_4) in sediments from the Santa Barbara Basin: Implications for paleoenvironmental changes during the past 35 ka. *Paleoceanography*, **24**, PA2224, DOI: 10.1029/2008PA001719.

Bloemendal J., King J.W., Hall F.R. and Doh S.-J., 1992. Rock magnetism of late Neogene and Pleistocene deep-sea sediments - relationship to sediment source, diagenetic processes and sediment lithology. *J. Geophys. Res.*, **97**, 4361–4375.

Brachfeld S., Barletta F., St-Onge G., Darby D. and Ortiz J.D., 2009. Impact of diagenesis on the environmental magnetic record from a Holocene sedimentary sequence from the Chukchi-Alaskan margin, Artic Ocean. *Global Planet. Change*, **68**, 100–114.

Canfield D.E. and Thamdrup B., 2009. Towards a consistent classification scheme for geochemical environments, or, why we wish the term 'suboxic' would go away. *Geobiology*, **7**, 385–392.

Chiang L., Vasiliev J., van Baak C., Krijsman W., Dekkers M.J., Roberts A.P., Gerald J.D.F., van Hoesnel A. and Winklhofer M., 2014. Identification and environmental interpretation of diagenetic and biogenic greigite in sediments: A lesson from the Messinian Black Sea. *Geochem. Geophys. Geosyst.*, **15**, 3612–3627.

Day R., Fuller M. and Schmidt P.V., 1977. Hysteresis properties of titanomagnetites:grain-size and compositional dependence. *Phys. Earth Planet. Inter.*, **13**, 260–267.

De Diego T.A., 1998. *Oxygen-Related Biofacies in Slope Sediments from the Western Gulf of California, Mexico*. MSc Thesis. Geological Sciences, University of Southern California, Los Angeles, CA, 132 pp.

Dinares-Turell J., Hoogakker B.A.A., Roberts A.P., Rohling E.J. and Sagnotti L., 2003. Quaternary climatic control of biogenic magnetite production and eolian dust input in cores from the Mediterranean Sea. *Palaeogeogr. Palaeoclimatol. Palaecol.*, **190**, 195–209.

Donegan D. and Shrader H., 1982. Biogenic and abiogenic components of laminated hemipelagic sediments in the central Gulf of California. *Mar. Geol.*, **48**, 215–237.

Douglas R., Gonzalez-Yajimovich O., Ledesma-Vazquez J. and Staines-Urias F., 2007. Climate forcing, primary production and the distribution of Holocene biogenic sediments in the Gulf of California. *Quat. Sci. Rev.*, **26**, 115–129.

Dunlop D.J., 1983. Viscous magnetization of 0.04-100 μm magnetites. *Geophys. J. R. Astr. Soc.*, **74**, 667–687.

Dunlop D.J., 2002. Theory and applications of the Day plot (Mrs/Ms versus Her/He) 1: Theoretical curves and tests using titanomagnetite data. *J. Geophys. Res.*, **107**, DOI: 10.1029 /2001JB000486.

Froelich P., Klinkhammer G.P., Bender M.L., Luedtke N.A., Heath G.R., Cullen D., Dauphin P., Hammond D., Hartman B. and Maynard V., 1979. Early oxidation of organic matter in pelagic sediments of the eastern equatorial Atlantic: suboxic diagenesis. *Geochim. Cosmochim. Acta*, **43**, 1075–1090.

Garming J.F.L., Bleil U. and Riedinger., 2005. Alteration of magnetic mineralogy at the sulfate-methane transition: Analysis of sediments from the Argentine continental slope. *Phys. Earth Planet. Inter.*, **151**, 290–308.

Goldhaber M.B. and Kaplan I.R., 1980. Mechanisms of sulfur incorporation and isotope fractionation during early diagenesis in sediments of the Gulf of California. *Mar. Chem.*, **9**, 95–143.

Gonzalez-Yajimovich O.E., Gorsline D.S. and Douglas R.G., 2007. Frequency and sources of basin floor turbidites in Alfonso Basin, Gulf of California, Mexico: Products of slope failures. *Sediment. Geol.*, **199**, 91–105.

Hayashida A., Hattori S. and Oda H., 2007. Diagenetic modification of magnetic properties observed in a piston core (MD01-2407) from the Oki Ridge, Japan Sea. *Paleogeogr. Paleoclimatol. Paleoecol.*, **247**, 65–73.

Helly J.J. and Levin L.A., 2004. Global distribution of naturally occurring marine hypoxia on continental margins. *Deep-Sea Res. Part I-Oceanogr. Res. Pap.*, **51**, 1159–1168.

Hofmann A.F., Peltzer E.T., Walz P.M. and Brewer P.G., 2011. Hypoxia by degrees: Establishing definitions for a changing ocean. *Deep-Sea Res. Part I-Oceanogr. Res. Pap.*, **58**, 1212–1226.

Hounslow M.W. and Maher B.A., 1999. Source of the climate signal recorded by magnetic susceptibility in Indian Ocean sediments. *J. Geophys. Res.*, **104**, 5047–5061.

Jackson M., Moskowitz B., Rosenbaum J. and Kissel C., 1998. Field-dependence of AC susceptibility in titanomagnetites. *Earth Planet. Sci. Lett.*, **157**, 129–139.

Karlin R., 1990. Magnetic mineral diagenesis in suboxic sediments at Bettis Site W-N, NE Pacific Ocean. *J. Geophys. Res.*, **95**, 4421–4436.

Karlin R. and Levi S., 1983. Diagenesis of magnetic minerals in Recent hemipelagic sediments. *Nature*, **303**, 327–330.

Karlin R. and Levi S., 1985. Geochemical and sedimentological control of the magnetic properties of hemipelagic sediments. *J. Geophys. Res.*, **90**, 10373–10392.

Kawamura N., Kawamura K. and Ishikawa N., 2008. Rock magnetic and geochemical analyses of surface sediment characteristic in deep ocean environments: A case study across the Ryukyu Trench. *Earth Planets Space*, **60**, 179–189.

Kawamura N., Ishikawa N. and Torii M., 2012. Diagenetic alteration of magnetic minerals in Labrador Sea sediments (IODP Sites U1305, U1306, and U1307). *Geochem. Geophys. Geosyst.*, **13**, Q08013 DOI: 10.1029/2012GC004213.

Kruiver P.P., Dekkers M.J. and Heslop D., 2001. Quantification of magnetic coercivity components by the analysis of acquisition curves of isothermal remanent magnetization. *Earth Planet. Sci. Lett.*, **189**, 269–276.

Leslie B.W., Lund S.P. and Hammond D.E., 1990a. Rock magnetic evidence for dissolution and authigenic growth of magnetic minerals in anoxic sediments from the California continental borderland. *J. Geophys. Res.*, **95(B4)**, 4437–4452.

Leslie B.W., Hammond D.E., Berelson W.M. and Lund S.P., 1990b. Diagenesis in anoxic sediments from the California continental borderland and its influence on iron, sulfur, and magnetite behavior. *J. Geophys. Res.*, **95(B4)**, 4453–4470.

Maher B.A. and Thompson R., 1999. *Quaternary Climates, Environments and Magnetism*. Cambridge University Press, Cambridge, U.K.

Miao X., Mason J.A., Swinehart J.B., Loope D.B., Hanson P.R., Goble R.J. and Liu X., 2007. A 10,000 year record of dune activity, dust storms, and severe drought in the central Great Plains. *Geology*, **35**, 119–122.

Molina-Cruz A., Pérez-Cruz L. and Monreal-Gómez M.A., 2002. Laminated sediments in the Bay of La Paz, Gulf of California: a depositional cycle regulated by pluvial flux. *Sedimentology*, **49**, 1401–1410.

Monreal-Gómez M.A., Molina-Cruz A. and Salas-de-León D.A., 2001. Water masses and cyclonic circulation in Bay of La Paz, Gulf of California, during June 1998. *J. Mar. Syst.*, **30**, 305–315.

Passier H.F., de Lange G.J. and Dekkers M.J., 2001. Magnetic properties and geochemistry of the active oxidation front and the youngest sapropel in the eastern Mediterranean Sea. *Geophys. J. Int.*, **145**, 604–614.

Pérez-Cruz L., 2006. Climate and ocean variability during mid-late Holocene recorded in laminated sediments from Alfonso Basin, Gulf of California, Mexico. *Quat. Res.*, **65**, 401–410.

Pérez-Cruz L., 2013. Hydrological changes and paleoproductivity in the Gulf of California during middle and late Holocene and their relationship with ITCZ and North American Monsoon variability. *Quat. Res.*, **79**, 138–151.

Pérez-Cruz L. and Urrutia-Fucugauchi J., 2009. Magnetic mineral study of Holocene marine sediments from the Alfonso Basin, Gulf of California - implications for depositional environment and sediment sources. *Geof. Int.*, **48**, 305–318.

Pérez-Cruz L. and Urrutia-Fucugauchi J., 2010a. Holocene laminated sediments from the southern Gulf of California: geochemical, mineral magnetic and microfossil study. *J. Quat. Sci.*, **25**, 989–1000, DOI: 10.1002/jqs.1386.

Pérez-Cruz L. and Urrutia-Fucugauchi J., 2010b. Characterization of distal turbidites in marine sedimentary sequences using magnetic mineral data and factor analysis of microfossil assemblages. *Stud. Geophys. Geod.*, **54**, 595–606.

Pike J. and Kemp A.E.S., 1997. Early Holocene decadal-scale ocean variability recorded in Gulf of California laminated sediments. *Paleoceanography*, **12**, 227–238.

Richter C., Hayashida A., Guyodo Y., Valet J.P. and Verosub K.L., 1999. Magnetic intensity loss and core diagenesis in long-core samples from the East Cortez Basin and the San Nicolas Basin (California borderland). *Earth Planets Space*, **51**, 329–336.

Roberts A.P., 2015. Magnetic mineral diagenesis. *Earth Sci. Rev.*, **151**, 1–47.

Roberts A.P., Chang L., Rowan C.J., Horng C.-S. and Florindo F., 2011. Magnetic properties of sedimentary greigite (Fe_3S_4): An update. *Rev. Geophys.*, **49**, RG10002.

Robinson S.G., Maslin A. and McCave I.M., 1995. Magnetic susceptibility variations in upper Pleistocene deep-sea sediments of the North Atlantic: Implications for ice rafting and paleocirculation at the last glacial maximum. *Paleoceanography*, **10**, 221–250.

Rowan C.J., Roberts A.P. and Broadbent T., 2009. Reductive diagenesis, magnetite dissolution, gregite growth and paleomagnetic smoothing in marine sediments: A new view. *Earth Planet. Sci. Lett.*, **277**, 223–235.

Tarduno J.A., 1995. Superparamagnetism and reduction diagenesis in pelagic sediments: Enhancement or depletion? *Geophys. Res. Lett.*, **22**, 1337–1340.

Urrutia-Fucugauchi J., 1981. Some observations on short-term magnetic viscosity behavior at room temperature. *Phys. Earth Planet. Inter.*, **26**, 1–5.

Verosub K.L. and Roberts A.P., 1995. Environmental magnetism: past, present and future. *J. Geophys. Res.*, **100**, 2175–2192.

Viau A.E., Gajewski K., Fines P., Atkinton D.E. and Sawada M.C., 2002. Widespread evidence of 1500 yr climate variability in North America during the past 14000 yr. *Geology* **30**, 455–458.

Vigliotti L., 1997. Magnetic properties of light and dark sediment layers from the Japan Sea: Diagenetic and paleoclimatic implications. *Quat. Sci. Rev.*, **16**, 1093–1114.

Worm H.U., 1998. On the superparamagnetic-stable single domain transition for magnetite, and frequency dependence of susceptibility. *Geophys. J. Int.*, **133**, 201–206.

Yamazaki T., Abdeldayem A.L. and Ikehara K., 2003. Rock-magnetic changes with reduction diagenesis in Japan Sea sediments and preservation of geomagnetic secular variation in inclination during the last 30,000 years. *Earth Planets Space*, **55**, 327–340.

Zheng Y., Kissel C., Zheng H.B., Laj C. and Wang K., 2010. Sedimentation on the inner shelf of the East China Sea: magnetic properties,diagenesis and paleoclimatic implications. *Mar. Geol.*, **268**, 34–42, DOI: 10.1016/j.margeo.2009.10.009.

Wilson T.R.S., Thomson J., Colley S., Hydes D.J., Higgs N.C. and Sørensen J., 1985. Early organic diagenesis: the significance of progressive subsurface oxidation fronts in pelagic sediments. *Geochim. Cosmochim. Acta*, **49**, 811–822.